Synchrotron SAXS Study of Phase-Separation Kinetics in a Poly(2-chlorostyrene)/Polystyrene Blend

Qicong Ying, Benjamin Chu,* Guangwei Wu, Kung Linliu, and Tong Gao

Department of Chemistry, State University of New York at Stony Brook, Stony Brook, Long Island, New York 11794-3400

Takuhei Nose and Mamoru Okada

Department of Polymer Chemistry, Tokyo Institute of Technology, Ookayama, Meguro-ku, Tokyo 152, Japan

Received February 3, 1993; Revised Manuscript Received August 2, 1993®

ABSTRACT: The concentration fluctuations in a poly(2-chlorostyrene)/polystyrene (P2ClS/PS) blend and their changes induced by temperature jumps were studied using time-resolved synchrotron small-angle X-ray scattering (SAXS). The virtual structure factor, which represents a formal extension of the one-phase equilibrium structure factor into the two-phase region, has been obtained from the mean-field static susceptibilities measured in the one-phase region. Three sets of measurements at different jump temperatures (from 140 °C to 156.87 °C, to 166.96 °C, and then to 179.91 °C) were performed. In the metastable region (142–167 °C) the experiments indicate that the initial kinetics can be described by the theory developed by Binder, with relaxation times of chain molecules being in a scale of minutes. The values are comparable with the results of the self-diffusion coefficient (on the order of $\sim 10^{-15}$ cm^2 s^{-1}) of poly(bromostyrene)/polystyrene blends measured in the molten state. In the small scattering wave vector q range the initial relaxation rates of concentration fluctuations increased with increasing q in accordance with theoretical predictions. However, the relaxation process did not clearly follow a simple exponential law. The relaxation rate became slower with increasing time. In the case of a deeper jump (at 179.91 °C), the relaxation rate changed its sign from positive to negative, with the concentration fluctuations growing and eventually leading to phase separation.

Introduction

The kinetics of the phase separation of polymer blends from the homogeneous phase to the two-phase region is an interesting subject of many theoretical[1-3] and experimental investigations.[4-8] Most analysis has been based on the original Cahn–Hilliard (C–H)[9] theory of spinodal decomposition of low molecular weight systems. During the initial stages of phase separation the C–H theory provides a satisfactory description for the time dependence of the light-scattering curve only in the range of the smallest scattering vector. Discrepancy from the behavior based on the C–H model has commonly been observed at higher q values. A conclusive argument for this discrepancy is not yet available. However, Cahn and Hilliard ignored nonlinear terms in the continuity equation and the effects of thermal fluctuations, and many important constraints of the continuity equation could be removed.[10] To improve on the C–H model, Cook[11] retained the linear approximation and included a thermal fluctuation term in equations which described the dynamics of demixing. Lately, on the basis of the Cook theory, Binder[3] derived equations that included the effects of thermal fluctuations for the time dependence of the structure factor of a polymer blend after a temperature jump. The evolution of the structure factor was described by a relaxation equation and a virtual structure factor.

In this paper, work was started with an investigation of the equilibrium concentration fluctuations in the one-phase region by synchrotron small angle x-ray scattering of a polymer blend sample, poly(2-chlorostyrene)/polystyrene (P2ClS/PS). The virtual structure factor was obtained from the measured static susceptibilities in the one-phase region that exhibited a mean field behavior. The kinetics of phase separation after temperature jumps were studied by time-resolved synchrotron SAXS measurements. The initial kinetics could be described by the Binder theory with relaxation times of chain molecules being in the order of minutes.

* Abstract published in *Advance ACS Abstracts*, October 1, 1993.

Experimental Section

Materials and Sample Preparation. Polystyrene with weight-average molecular weight $M_w = 3.5 \times 10^4$ and narrow molecular weight distribution $M_w/M_n < 1.06$ was purchased from Pressure Chemical Co. Poly(2-chlorostyrene) was radically polymerized in toluene and fractionated by the precipitation method using toluene and methanol as the solvent and the precipitant, respectively. M_w/M_n and M_w were determined by gel permeation chromatography and light scattering to be 1.09 and 1.09×10^5, respectively. Films of the P2ClS/PS blend (named sample G) with composition $W_{PS}/W_{P2ClS} = 59.9/40.1$ (by weight) were prepared according to the procedure described in detail elsewhere.[12,13]

SAXS Measurements. SAXS experiments were conducted at the SUNY X3A2 Beamline, National Synchrotron Light Source, Brookhaven National Laboratory, using a modified Kratky collimator[14] and a one-dimensional Braun detector, Type-OED 50/straight. The X-ray wavelength was set at 0.154 nm. The sample holder was set in a hot stage, which consisted of two heating brass blocks independently controlled to ±0.02 °C over a temperature range from 60 to 215 °C by two independent precision temperature controllers. The blend sample underwent a quick temperature jump by using a manually controlled pneumatic piston pushing the slide holding the sample holder from the preheated block to the measurement block, which was set at the desired measuring temperature. After a temperature jump, the equilibration of temperature took place in 2–3 min depending on the temperature difference (ΔT) between the two blocks (in this work $\Delta T < 40$ °C), and each scattering measurement was collected for 50-s periods during the first 3000 s and then collected for 500-s periods during the last 3000–5000 s. All SAXS profiles were corrected for incident X-ray intensity fluctuations, sample and Kapton film attenuations, and background parasitic scattering.

Results and Discussion

I. Evaluation of the Virtual Structure Factor. In the one-phase region, the structure factor $S(q)$ (of a

0024-9297/93/2226-5890$04.00/0

homogeneous polymer mixture) ($q \equiv |q| = (4\pi/\lambda)\sin(\theta/2)$, where θ and λ are the scattering angle and the X-ray wavelength, respectively) can be described by the random-phase approximation (RPA)[15]

$$S^{-1}(q) = (N_A\phi_A)^{-1}f_D^{-1}(q^2R_A^2) + (N_B\phi_B)^{-1}f_D^{-1}(q^2R_B^2) - 2\chi \quad (1)$$

$$f_D(q^2R_i^2) = (2/q^2R_i^2)[1 - (1 - \exp(-q^2R_i^2))/q^2R_i^2] \quad (2)$$

$$I(q) \propto S(q) \quad (3)$$

where N_i, ϕ_i, and R_i are respectively the degree of polymerization, the volume fraction, and the radius of gyration of component i (i = A, B). χ is the Flory–Huggins interaction parameter of local monomer–monomer interactions, $I(q)$ is the scattered intensity. $f_D(q^2R_i^2)$ denotes the Debye structure factor for noninteracting ideal chains. In the small q range eq 1 could be rewritten in an approximate expression

$$S^{-1}(q) \cong (N_A\phi_A)^{-1}[1 - (q^2R_A^2/3)]^{-1} + (N_B\phi_B)^{-1}[1 - (q^2R_B^2/3)]^{-1} - 2\chi \cong [(N_A\phi_A)^{-1} + (N_B\phi_B)^{-1}][1 + (q^2R_g^2/3)] - 2\chi \quad (4)$$

where the mean radius of gyration R_g is defined by

$$R_g^2 = [(N_A\phi_A)^{-1} + (N_B\phi_B)^{-1}]^{-1}[R_A^2/(N_A\phi_A) + R_B^2/(N_B\phi_B)] \quad (5)$$

After a temperature jump, the equilibrium structure factor is changed. Corresponding to the treatment of Cook[11] for the small-molecule system, Binder[3] derived the time dependence of the structure factor $S(q,t)$

$$S(q,t) = S_\chi(q) + [S(q,0) - S_\chi(q)]\exp(-2\tau_q^{-1}t) \quad (6)$$

where τ_q^{-1} [$=q^2\Lambda(q)\,S_\chi^{-1}(q)$, with $\Lambda(q)$ being a Fourier transform of the (mean) Onsager coefficient] is the relaxation rate of concentration fluctuations. $S_\chi(q)$ is the structure factor in the limit of $t \to \infty$

$$S(q,t)_{t\to\infty} = S_\chi(q) \quad (7)$$

In the one-phase region, $S_\chi(q)$ constitutes the equilibrium structure factor ($S(q)$); in the spinodal region $S_\chi(q)$ corresponds to a virtual structure factor. Equation 6 describes the phase separation in its initial stages. Under the condition of weak symmetry, i.e., $N_A \simeq N_B$, Binder[3] proposed the following equation:

$$\tau_q^{-1} \simeq (6/\tau_R)q^2R_m^2(1 - (\chi/\chi_s)f_D(q^2R_m^2)) \quad (8)$$

Here, τ_R specifies the time required by a chain molecule to diffuse over a length comparable to its own size and R_m [$=[(1 - \phi_A)R_A^2 + \phi_AR_B^2]^{1/2}$] denotes a mean radius of gyration. χ_s is the Flory–Huggins interaction parameter at the mean-field spinodal temperature.

The virtual structure factor, being a consequence of taking into account the thermal fluctuations, cannot be determined directly by static measurements. Nevertheless, the virtual structure factor permits us to explore the influence of thermal fluctuations in a polymer system. In 1986, Okada and Han[16] calculated the virtual structure factor by a nonlinear fitting of time-dependent scattered intensity data. As expected from theory the change of temperature could result in a parallel shift of $(1/I(q,t)) \sim q^2$ curves. When absolute scattered intensity $I(q,t) \propto S(q,t)$, Meier and Strobl[17] calculated the virtual structure factor from $dI^{-1}(q,t)/dT$ estimated from the experimental

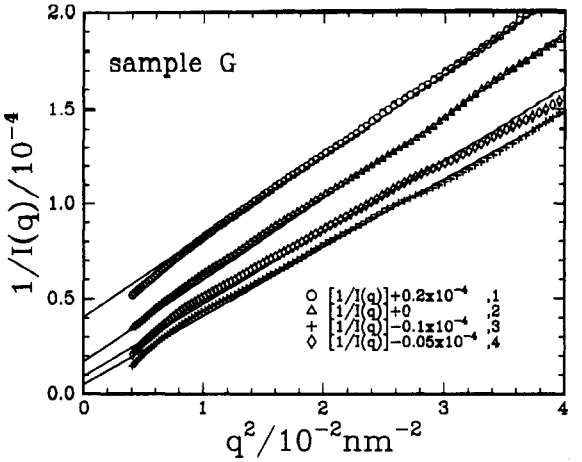

Figure 1. Plots of $I^{-1}(q)$ vs q^2 for sample G at different temperatures. Curve 1: T = 134.90 °C. Curve 2: T = 139.97 °C. Curve 3: T = 141.99 °C. Curve 4: T = 144.07 °C.

data. However, a parallel shift in the $I^{-1}(q,t) \sim q^2$ curve with temperature change is not the case in our measurements, especially for the temperatures in the vicinity of T_c. Figure 1 shows an Ornstein–Zernicke plot of $I^{-1}(q,t)$ vs q^2 of sample G at different temperatures. Curves 1 and 2 measured at 134.90 and 139.97 °C, respectively, showed almost the same slope. For curves 3 (at 141.99 °C) and 4 (at 144.07 °C) measured at temperatures very close to the phase-separation temperature, the slopes seemed to change with temperature.

Evaluation of the virtual structure factor in this work is based on eq 4. From the SAXS experiments, the fundamental data measured are scattering intensities $I(q)$. The relation between the absolute intensities and the scattering function $S(q)$ shown in eq 4 is given by

$$I(q) = \Delta\rho^2v_mS(q) \quad (9)$$

where $\Delta\rho$ denotes the electron density difference between the two mixed components, and v_m is the volume of the monomer unit. In our measurements the scattered intensities were represented in relative units, which are related to the absolute scattered intensity, as $I_R(q) = AI(q)$, with A being a proportionality constant. Thus, eq 9 could be rewritten as

$$I_R^{-1}(q) = FS^{-1}(q) \quad (10)$$

where F ($=1/(A\Delta\rho^2v_m)$) is a constant making the units on both sides of eq 10 consistent. The factor F should be virtually independent of temperature but dependent on the unit of $I_R(q)$ used and on the character of the sample. To find out constant F from SAXS experiments measured in relative scale is an important step in evaluating the virtual structure factor. In the one-phase region, based on eq 4 when $q^2R_g^2 < 1$ and $q \to 0$, the Debye structure factor $f_D(q^2R_g^2)$ can be written as $1 - (1/3)q^2R_g^2 \simeq 1$, and the thermal equilibrium structure factor at $q = 0$ is then given by

$$S^{-1}(q=0) = [(N_A\phi_A)^{-1} + (N_B\phi_B)^{-1}] - 2\chi(T) \quad (11)$$

Therefore

$$I_R^{-1}(0) = F\{[(N_A\phi_A)^{-1} + (N_B\phi_B)^{-1}] - 2\chi(T)\} \quad (12)$$

$\chi(T)$ can be evaluated by using the correlation length $\xi(T)$ measured in the one-phase region by using the relation

$$\chi(T) = \chi_s - (R_g^2/6)[(N_A\phi_A)^{-1} + (N_B\phi_B)^{-1}]\xi(T)^{-2} \quad (13)$$

and χ_s can be calculated from the Flory–Huggins equation[18]

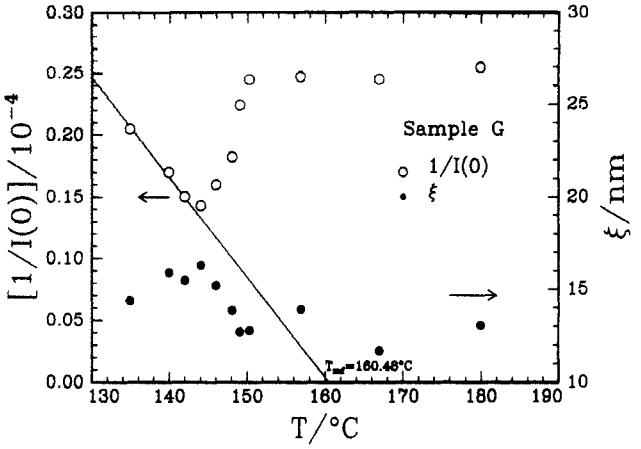

Figure 2. Plot of $I^{-1}(0)$ vs T and ξ vs T for sample G.

$$\chi_s = (v_0/2)[(1/N_A\phi_A v_A) + (1/N_B\phi_B v_B)] \quad (14)$$

where v_0 [$=\phi_A v_A + \phi_B v_B$] is the molar volume of a reference unit of a polymer blend, with v_A and v_B being the molar volumes of monomers A and B, respectively. Thus, the constant F can be determined by eq 12, if N_i, ϕ_i, $\chi(T)$, and $I_R^{-1}(0)$ are known. In the spinodal region, eqs 10 and 12 with known F are inserted into eq 4, which then becomes

$$\begin{aligned} I_{\chi R}^{-1}(q) &= F\{[(N_A\phi_A)^{-1} + (N_B\phi_B)^{-1}][1 + (q^2R_g^2/3)] - 2\chi\} \\ &= F\{[(N_A\phi_A)^{-1} + (N_B\phi_B)^{-1}] - 2\chi\} + F[(N_A\phi_A)^{-1} + \\ &\qquad (N_B\phi_B)^{-1}](q^2R_g^2/3) \\ &= I_R^{-1}(q=0) + F[(N_A\phi_A)^{-1} + \\ &\qquad (N_B\phi_B)^{-1}][f_D^{-1}(q^2R_g^2) - 1] \quad (15) \end{aligned}$$

The virtual structure factor $I_{\chi R}(q)$ (or $S_\chi(q)$) can be determined from eq 15, if $I_R^{-1}(0)$ are known.

Figure 2 shows a plot of $I^{-1}(0)$ vs T where the subscript R in $I_R^{-1}(0)$ has been dropped because in this work all the scattered intensities were determined on a relative scale. In the temperature range of 134.90–141.99 °C, the results at three temperatures exhibited essentially a mean-field behavior ($I^{-1}(0) \propto T$). At higher temperatures a kink in the curve of $I^{-1}(0)$ vs T appeared and then the scattered intensities and correlation lengths changed slowly with increasing temperature up to 180 °C. The decrease in the scattered intensity after the kink was probably due to the facts that the polymer blend was now in the two-phase region and the large domain size during the initial stages of phase separation could occur at scattering angles smaller than the accessible small scattering angular range in the present SAXS setup. The estimated mean-field spinodal decomposition temperature T_{mf} was 160.48 °C. In the temperature region (156.87, 166.96, and 179.91 °C), the values of $I(0)$ could be obtained by extrapolating the scattering data measured in the one-phase region into the two-phase region according to the mean-field behavior. Such a plot is shown in Figure 3. In the mean-field region the temperature dependence of the correlation length was found to be $\xi^{-2}(T) = 24.77/T - 0.05583$, with ξ and T expressed in nanometers and Kelvin, respectively. The actual values used in computing the constant F above are listed in Table I. The F values calculated from three temperatures (134.90, 139.97, and 141.99 °C) in the mean-field region behaved as constants and were independent of temperature, $F = 0.029 \pm 0.002$ (for $I(q)$ measured in counts/1000 s).

The structure factors of sample G, which were calculated from eq 15, are presented in Figure 4 as a plot of $I_\chi^{-1}(q)$ vs q^2 at different temperatures. At temperatures below

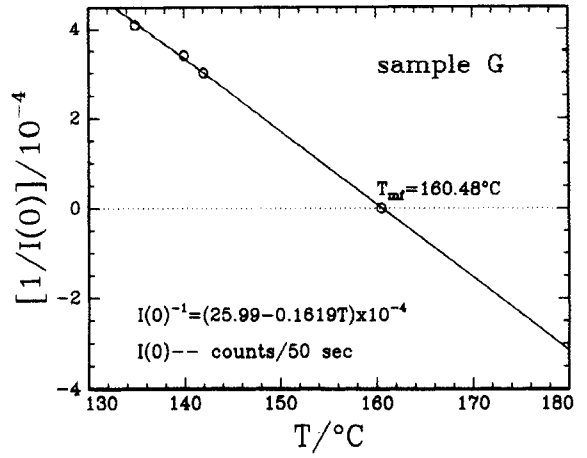

Figure 3. Plot of $I^{-1}(0)$ vs T for sample G at T = 134.90, 139.97, and 141.99 °C.

Table I. Sample G

T (K)	$I^{-1}(0)/10^{-4}$ (counts/1000 s)	$\xi(T)$ (nm)	$\xi(T)^a$ (nm)	$\chi(T)^b/10^{-3}$	F
408.05	0.205	14.4	14.3	3.76_2	0.031
413.12	0.170	15.9	15.6	3.81_8	0.031
415.14	0.150	15.5	16.1	3.80_4	0.026

[a] Calculated from $\xi^{-2}(T) = 24.77/T - 0.05583$. [b] Calculated from eq 13.

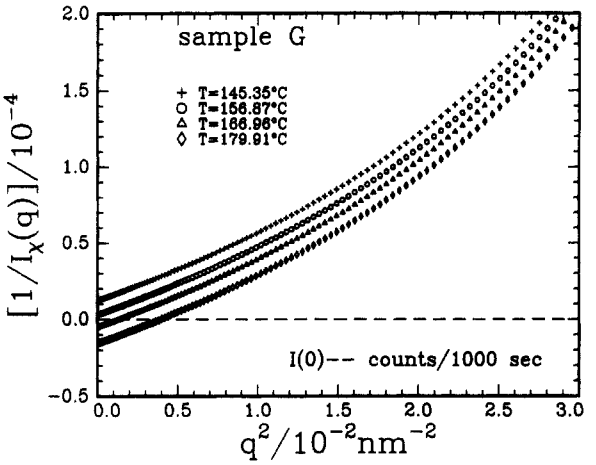

Figure 4. Plots of $I_\chi^{-1}(q)$ vs q^2 for sample G at different temperatures.

T_{mf}, e.g., at T = 145.35 °C (pluses) and 156.87 °C (hollow circles), the curves exhibited an equilibrium situation, i.e., $I_\chi^{-1}(q)$ was positive for all q values of our experiments and very close to the spinodal line, where $I_\chi^{-1}(q=0) = 0$. From the results of static measurements the temperatures 145.35 and 156.87 °C located the blend in the metastable region. The closeness to the spinodal line could be visualized by the closeness of the curves to $I_\chi^{-1}(q=0) = 0$. At temperatures higher than T_{mf}, i.e., at T = 166.96 °C (hollow triangles) and 179.91 °C (hollow diamonds), the blend was in the spinodal region, where the $I_\chi^{-1}(q)$ values became negative for $q < q_c$ and positive for $q > q_c$. q_c denoted a critical q value at which $I_\chi^{-1}(q) = 0$. At T = 166.96 °C, $q_c \sim 0.04$ nm^{-1}; at T = 179.91 °C, $q_c \sim 0.07$ nm^{-1}. The P2ClS/PS blend has a lower critical solution temperature. Thus, q_c shifted to higher values with increasing temperature. The q_c values were smaller than or at the lower margin of the scattering vector which could be reached by the present SAXS setup.

II. Relaxation Time of a Chain Molecule and Phase-Separation Kinetics in the Two-Phase Region. Two temperature jumps were performed from tempera-

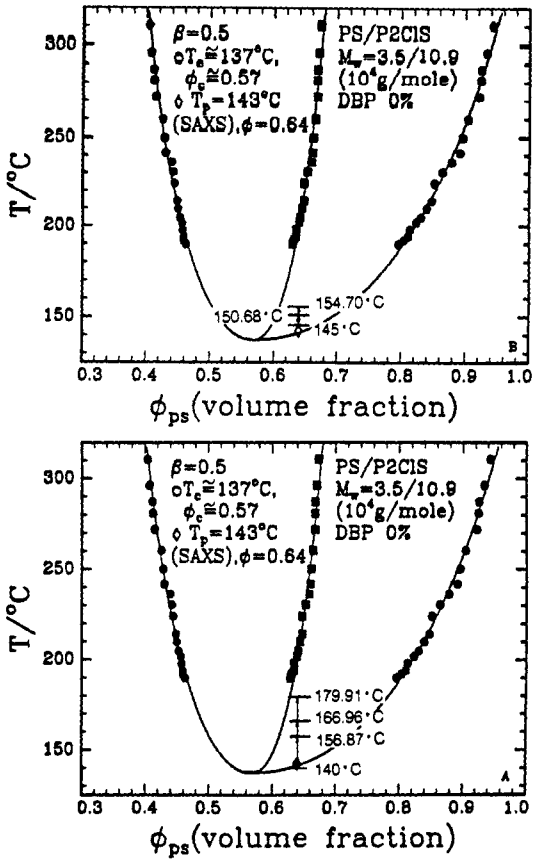

Figure 5. Binodal curves of a P2ClS/PS blend (sample G). The arrows show the temperature regions where jump measurements were performed: (A) from 140 °C → 156.87 °C (total time 7860 s) → 166.96 °C (total time 7800 s) → 179.91 °C (total time 4848 s); (B) from 145 °C (total time 4878 s) → 150.68 °C (total time 7785 s) → 154.70 °C (total time 7245 s). Filled circles denote the data determined by the centrifugal method; filled rectangles denote concentrations which specify the midpoint of the concentrations at the two coexisting phases. The curve which passes through the filled rectangles represents an arithmetic mean of the coexisting concentrations of the fitting curve.

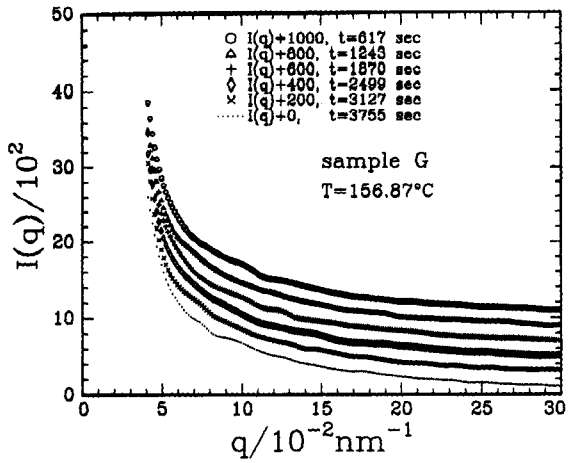

Figure 6. Time-dependent SAXS curves measured at $T = 156.87$ °C.

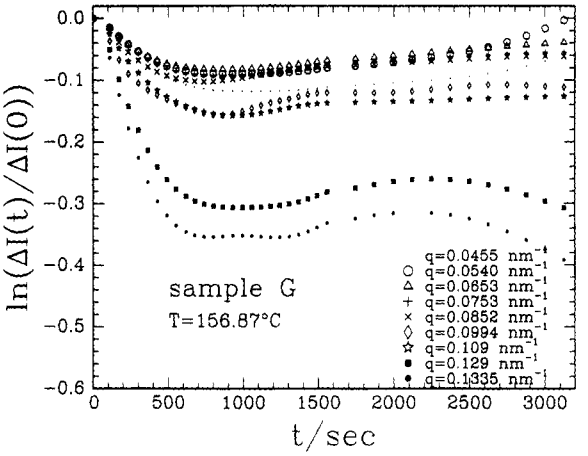

Figure 7. Plots of $\ln[(I(q,t) - I_\chi(q))/(I(q,0) - I_\chi(q))]$ vs time t at different q values, at $T = 156.87$ °C.

tures in the one-phase region to those in the two-phase region, and the time evolution of the scattered intensity was measured. As a supplement to the usual single step jump, we carried out stepwise temperature jumps in the metastable and the unstable regions. The validity of the linearized theory was tested by analyzing the phase-separation change induced by the second jump. The time sequence was accomplished such that the phase separation that was initiated by the first jump was still in the early stage when the second jump was made. Two sets of successive temperature jump measurements were performed: (1) Temperature was jumped from 140 to 156.87 °C (at this temperature the sample was kept for 7860 s), then jumped to 166.96 °C (the sample was kept for 7800 s), and finally jumped to 179.91 °C. (2) Temperature was jumped from 145 to 150.68 °C (the sample was kept for 7785 s) and then jumped to 154.70 °C. Figure 5 shows the phase diagram of sample G, where the corresponding schemes of two separate sets of temperature jumps were indicated by arrows. Figure 6 shows the time-dependent scattering curves measured at 156.87 °C.

According to Binder's theoretical prediction,[19] there are various regions in the metastable regime: very close to the critical temperature T_c, there exists a non-mean-field critical regime, where the transition from nucleation to spinodal decomposition is smeared out and the spinodal decomposition is highly nonlinear even in the earliest stages after a temperature jump (or quench). Further away from T_c, the polymer blend should experience a crossover from the non-mean-field critical regime to a mean-field critical regime; the crossover occurs at $r^d(1 - T/T_c)^{2-d/2} \approx 1$ (or $N^{d/2-1}(1 - T/T_c)^{2-d/2} \approx 1$) only for dimension $d > 2$ (or $d = 3$),[19] where r is defined as the range of interaction. The region between the classical nucleation (near the coexistence curve) and the spinodal nucleation (near the spinodal) is characterized by very high nucleation barriers, and a treatment based on the linearized theory of spinodal decomposition should be valid. The values of $N^{0.5}(1 - T_c/T)^{0.5}$ estimated from the data of the metastable conditions studied, where $T_c = 410.15$ K, $T = 423.83, 427.85$, and 430.02 K, and $N = (N_{PS}N_{P2ClS})^{1/2} = 514$, were larger than 1 ($\approx 4$–5). Therefore, the metastable region studied in the present work is in the critical regime of mean-field behavior. The validity of the linearized theory could be tested by analyzing the experimental data of phase-separation change induced by the temperature jumps.

With the virtual structure factor $I_{\chi R}(q)$ determined from eq 15 by the procedure described in section I, the relaxation rate τ_q^{-1} can be evaluated from eqs 6 and 10. According to the linearized theory, the plot of $\ln(\Delta I(q,t)/\Delta I(q,0))$ versus t, where $\Delta I(q,t) = I(q,t) - I_\chi(q)$ and $\Delta I(q,0) = I(q,0) - I_\chi(q)$, shows a linear relation, and τ_q^{-1} is determined as its slope. Such plots are shown in Figures 7–9, where the first collected data after the temperature jump were taken as $I(q,0)$. The plots obviously show a curvature even in the very early period for all three different temperatures; the relaxation process does not follow a simple exponential law in the investigated q range. This fact was also observed by Strobl et al.[20,21] in studying the structure relaxation after a temperature jump in their SAXS study on the PS/

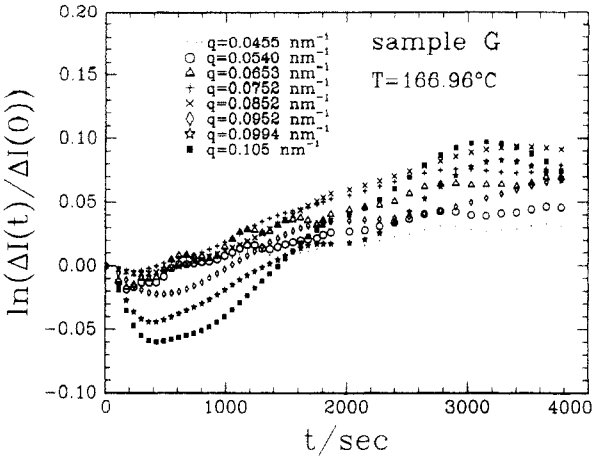

Figure 8. Plots of $\ln[(I(q,t) - I_\chi(q))/(I(q,0) - I_\chi(q))]$ vs time t at different q values, at T = 166.96 °C.

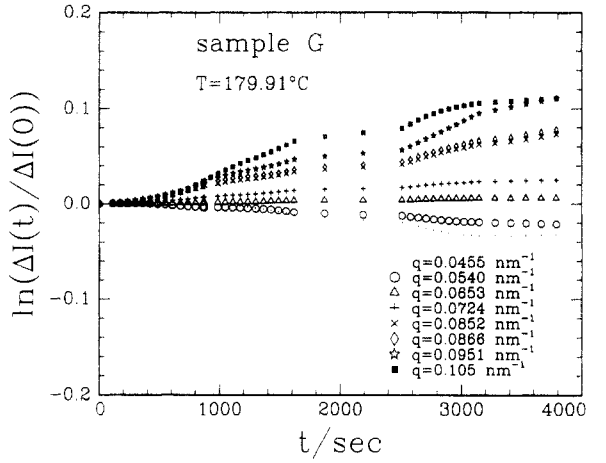

Figure 9. Plots of $\ln[(I(q,t) - I_\chi(q))/(I(q,0) - I_\chi(q))]$ vs time t at different q values, at T = 179.91 °C.

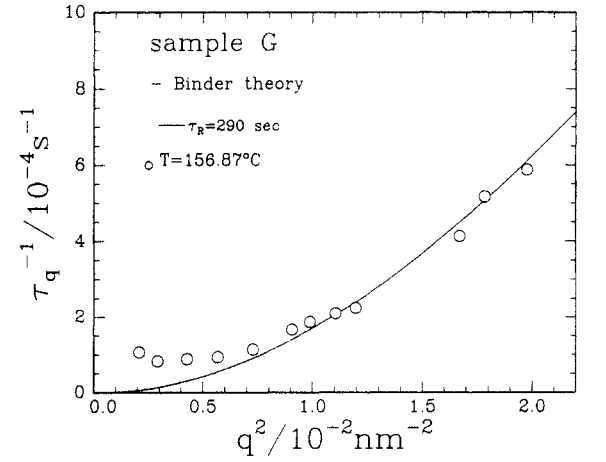

Figure 10. Plot of relaxation rate vs q^2 and fitting with the Binder theory, at T = 156.87 °C. $R_{m,cal} = [(1-\phi_A)R_A^2 + \phi_A R_B^2]^{1/2}$ = 7.45 nm with ϕ_A = 0.6429, R_A = 5.60 nm, R_B = 8.30 nm, and $R_{m,fit}$ = 7.40 nm.

poly(styrene-*co*-bromostyrene) blend. The observations make a contrast with the fact that the exponential behavior is commonly observed by light scattering measurements. However, on the basis of the initial slope of the relaxation curves, the initial relaxation times could be obtained and are presented in Figures 10 and 11. All initial τ_q values are positive. The solid lines are fits of the data using the Binder equation (eq 8) with τ_R and R_m as fitting parameters. $\chi(T)$ and χ_s were calculated from eqs 12 and 14, respectively. The best fitting values are τ_R = 750 s at 150.68 °C and τ_R = 290 s at 156.87 °C.

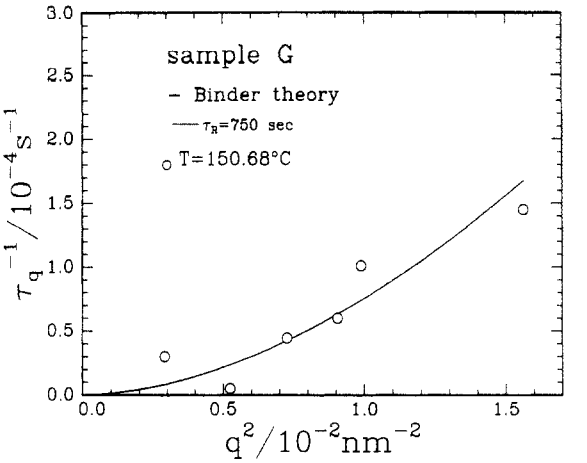

Figure 11. Plot of relaxation rate vs q^2 and fitting with the Binder theory, at T = 150.68 °C. $R_{m,cal} = [(1-\phi_A)R_A^2 + \phi_A R_B^2]^{1/2}$ = 7.45 nm with ϕ_A = 0.6428, R_A = 5.60 nm, R_B = 8.30 nm, and $R_{m,fit}$ = 7.40 nm.

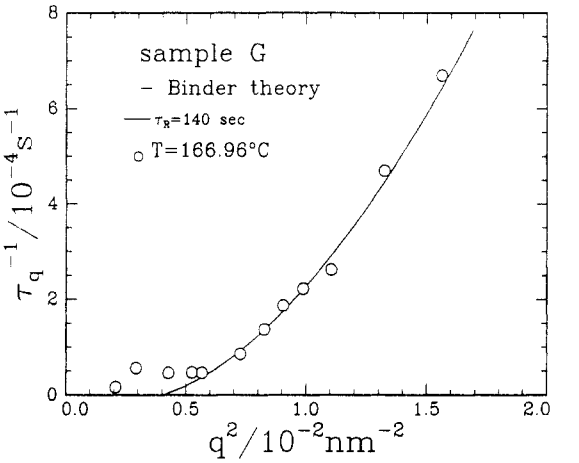

Figure 12. Plot of relaxation rate vs q^2 and fitting with the Binder theory, at T = 166.96 °C. $R_{m,cal} = [(1-\phi_A)R_A^2 + \phi_A R_B^2]^{1/2}$ = 7.45 nm with ϕ_A = 0.6430, R_A = 5.60 nm, R_B = 8.30 nm, and $R_{m,fit}$ = 6.14 nm.

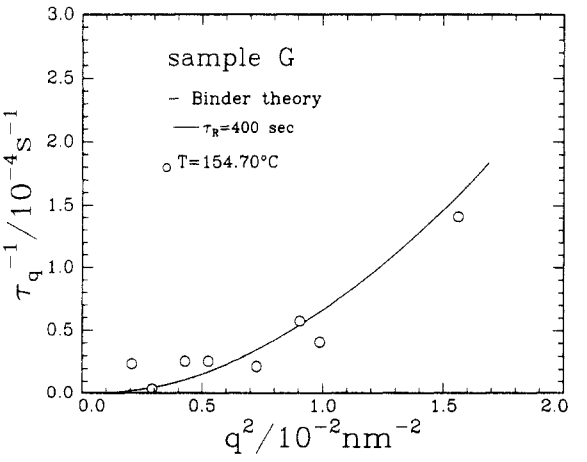

Figure 13. Plot of relaxation rate vs q^2 and fitting with the Binder theory, at T = 154.70 °C. $R_{m,cal} = [(1-\phi_A)R_A^2 + \phi_A R_B^2]^{1/2}$ = 7.45 nm with ϕ_A = 0.6429, R_A = 5.60 nm, R_B = 8.30 nm, and $R_{m,fit}$ = 6.30 nm.

The same data analysis was applied to the data from the stepwise temperature jumps. The initial relaxation times were evaluated by the same procedure as mentioned above. Fitting of eq 8 also appeared satisfactory, as shown in Figures 12 and 13. The relaxation time τ_R decreased with increasing temperature and was consistent with those evaluated for the single-step jumps. Under the present

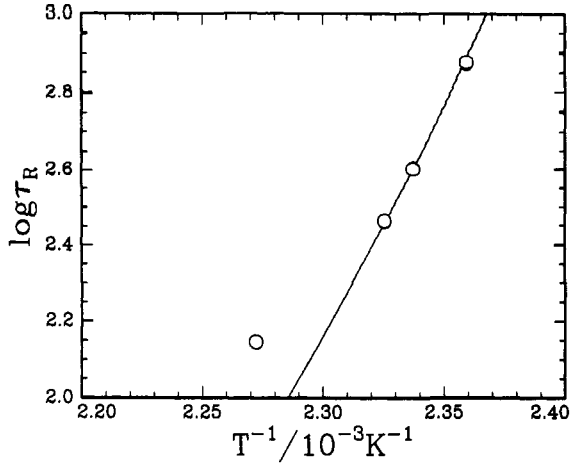

Figure 14. Plot of log τ_R versus $1/T$.

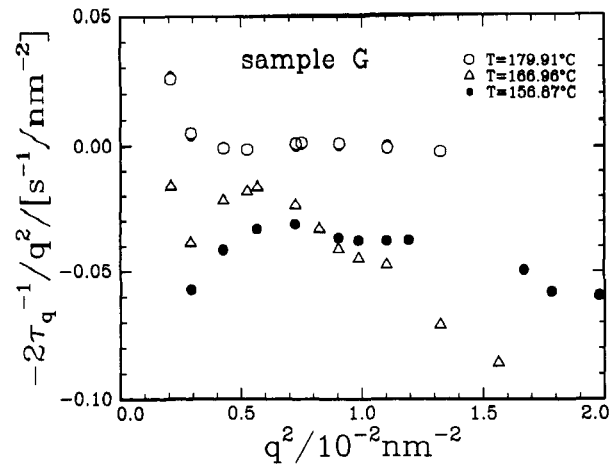

Figure 15. Plot of $-2\tau_q^{-1}/q^2$ vs q^2 at different temperatures.

condition the phase-separation kinetics after a jump from the metastable state appeared to be similar to the single-step jump from a one-phase homogeneous state, whereas the result of the jump from temperature 166.96 °C to the highest temperature 179.91 °C was different. We could not find a reasonable τ_R value. The results for the temperature (166.96 °C) in the unstable region appeared to be consistent with eq 8. However, the data fitting also showed a negative part for one of the curves at low q values, as had already been shown by Meier et al.[17] In our case no data point of negative relaxation time could be obtained.

For a system where the interaction term could not be neglected, Benmouna et al.[22] suggested that the relaxation time τ_0 (or τ_R) could be represented generally by

$$\tau_R = D_c^{-1} R_g^2 \tag{16}$$

where D_c is the self-diffusion coefficient of the center of mass. For the P2ClS/PS blend sample G, the mean radius of gyration $R_g \simeq 6.90$ nm. Substitution of $\tau_R = 290$ and 750 s into eq 16 gives $D_c = 1.6 \times 10^{-15}$ and 6.3×10^{-16} cm^2 s^{-1}, respectively. According to Eu and Ullman,[23] the self-diffusion coefficients of the PS/poly(bromostyrene) blend with molecular weights ranging from 3×10^4 to 1×10^5 evaluated from the SAXS measurements were on the order of 10^{-15}–10^{-16} cm^2 s^{-1}. The same order of the self-diffusion coefficient was found for the poly(deuteriostyrene)/poly(xylenyl ether) blend (PDS/PXE) with $M_{w,PDS} = 100\,000$ and $M_{w,PXE} = 44\,000$ measured by the SANS method.[24] Those results support the validity of our analysis.

The temperature dependence of τ_R could also be represented by plots of log τ_R versus $1/T$ as shown in Figure 14. The data point from the highest temperature 166.96 °C deviated from the other three points, which might be due to a decrease in precision in the τ_R determination at high temperatures in the unstable region. The apparent activation energy evaluated from the three data points at lower temperatures in the metastable region yielded a value 2.3×10^5 J/mol, which was in good agreement with 2.4×10^5 J/mol, a value estimated by the WLF equation with the constants C_1 and C_2 for polystyrene. Namely, the WLF equation

$$\log\left[\frac{\tau_R(T)}{\tau_R(T_g)}\right] = \frac{-C_1(T - T_g)}{C_2 + (T - T_g)} \tag{17}$$

gives the activation energy ΔH as

$$\Delta H = \frac{2.303RC_1C_2T^2}{(C_2 + T - T_g)^2} \tag{18}$$

where R is the gas constant and T is the absolute temperature.[25] The activation energy at 154.70 °C was calculated from eq 18, with $C_1 = 13.3$ and $C_2 = 47.5$ for PS based on viscoelastic measurements[26] and $T_g = 106$ °C for the present blend.[12] A curve of the WLF equation with the same parameters was drawn in Figure 14, where the following equation derived from eq 17 was used and the reference temperature T_r was taken to be 154.70 °C.

$$\log\left[\frac{\tau_R(T)}{\tau_R(T_r)}\right] = \frac{-C_1C_2(T - T_r)}{(C_2 + T_r - T_g)(C_2 + T - T_g)} \tag{19}$$

Agreement between experimental data and the calculated curve was unexpectedly good except the datum at the highest temperature in the unstable region.

In the kinetic study, the parameter $-\tau_q^{-1}$ is usually defined as the growth rate $R(q)$, which has a maximum at $q = q_{max} = q_c/\sqrt{2}$, and a linear relationship should appear in a plot of $R(q)/q^2$ vs q^2. As the kinetic measurements were performed in the metastable region, the q_c values might be too small to achieve an observable q_{max} experimentally. Furthermore, no linear relationship could be found in a plot of $2R(q)/q^2$ vs q^2 for the data sets measured at different jump temperatures, as already mentioned in previous studies.[4,27] Yet, Figure 15 shows that the $R(q)$ values at fixed q increased from negative toward positive with increasing temperature. At $T = 156.87$ °C, all $R(q)$ ($t \to 0$) values were negative, indicating that the fluctuations did not grow but decayed with a relaxation time τ_q and the system remained stable to concentration fluctuations at those wavevectors. There was a region of q in which $R(q)$ was positive, implying that the concentration fluctuations would grow and eventually lead to phase separation. In the metastable region, the phase separation developed slowly when compared with what happened in the spinodal region. Let $R(q,t) = R_{app}(q)$; Figures 16 and 17 show plots of $R_{app}(q)/q^2$ vs q^2 at different times. At $T = 156.87$ °C, which sets the blend in the metastable region, the values of $R_{app}(q)$ increased with increasing time up to 3755 s as shown in Figure 16 but still kept negative values within this time period. According to measurement rerults the metastable phase remained stable at least with $t <$ 7800 s. At $T = 166.96$ °C, in the small q region the values of $R_{app}(q)$ at fixed q values changed their sign from negative to positive at $t \geq 700$ s as shown in Figure 17, implying that the phase separation could occur over the q range of our measurements at $t > 700$ s after the blend was jumped to this temperature region from 156.87 °C. At $T = 179.91$ °C, $R(q)$ showed positive values, the blend was in the unstable region.

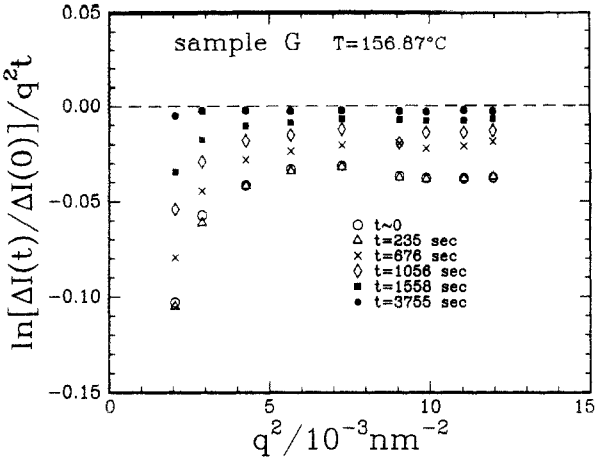

Figure 16. Plots of $\ln[\Delta I(t)/\Delta I(0)]/q^2t$ vs q^2 for sample G at jump temperature 156.87 °C.

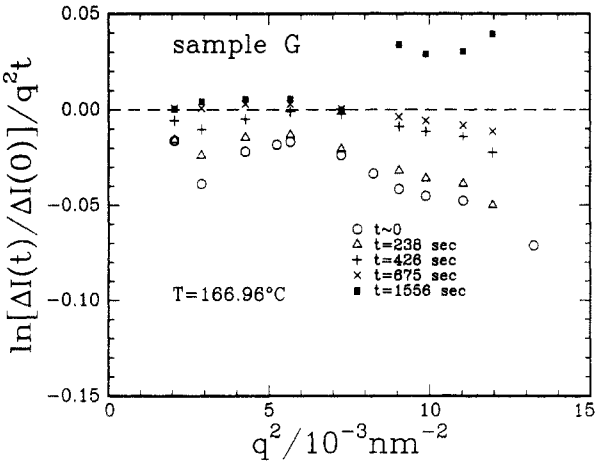

Figure 17. Plots of $\ln[\Delta I(t)/\Delta I(0)]/q^2t$ vs q^2 for sample G at jump temperature 166.96 °C.

Conclusions

In this study, we have demonstrated that the virtual structure factor can be evaluated from the static susceptibilities measured in the one-phase region where the blend obeyed the mean-field behavior. The $I_\chi^{-1}(q)$ curves, which were found from four different temperatures, 145.35, 156.87, 166.96, and 179.91 °C, in the two-phase region, followed exactly the characters that were predicted by the random-phase approximation. From static susceptibility measurements, we know that the temperatures 145.35 and 156.87 °C set the blend (sample G) in the metastable region (as shown in Figure 5), and the $I_\chi^{-1}(q)$ curves we found show positive values for all q and are very close to the spinodal line, where $I_\chi^{-1}(=0) = 0$. In the spinodal region at T = 166.96 and 179.91 °C, where q_c exists, $I_\chi(q)$ becomes negative for $q < q_c$.

In the metastable region the initial kinetics can be described by the Binder equation (eq 8), and the relaxation time τ_R for chain molecules is on the order of minutes (τ_R = 290 s at T = 156.87 °C; τ_R = 140 s at T = 166.96 °C). The τ_R value is comparable with the results from the self-diffusion coefficient (on the order of $\sim 10^{-15}$/cm^2 s^{-1}) of PBrS/PS and PDS/PXE blends. The P2ClS/PS blend system has a lower critical solution temperature. The growth rate $R(q)$ showed different temperature-dependent behavior in three different temperature regions. In the metastable region, at T = 156.87 °C, all $R(q)$ ($t \to 0$) values were negative, indicating that the system remained stable to concentration fluctuations at those wavevectors. At T = 166.96 °C and in the small q region the values of $R(q)$ at fixed q values were increasing toward the positive, implying that the phase separation could occur over the q range of our measurements at a certain time after the blend was jumped to this temperature region. At T = 179.91 °C, $R(q)$ showed positive values and the blend was in the unstable region.

Acknowledgment. We gratefully acknowledge the support of this project by the Department of Energy (Grants DEFG0286ER45237A005 and DEFG-0589ER75515), the SUNY Beamline (Grant DEFG-0286ER45321A005) at the National Synchrotron Light Source, Brookhaven National Laboratory, and the National Science Foundation (Grant INT8815115). B.C. acknowledges a fellowship from the Japan Society for the Promotion of Science.

References and Notes

(1) de Gennes, P.-G. *J. Chem. Phys.* **1980**, *72*, 4756.
(2) Pincus, P. *J. Chem. Phys.* **1981**, *75*, 1996.
(3) Binder, K. *J. Chem. Phys.* **1983**, *79*, 6387; *Colloid Polym. Sci.* **1987**, *265*, 273.
(4) Nose, T. *Phase Transitions* **1987**, *8*, 245.
(5) Briber, R. M.; Bauer, J. *Macromolecules* **1991**, *24*, 1899.
(6) Tanaka, H.; Hasegawa, H.; Hashimoto, T. *Macromolecules* **1991**, *24*, 240.
(7) Hasegawa, H.; Sakurai, S.; Takenaka, M.; Hashimoto, T.; Han, C. C. *Macromolecules* **1991**, *24*, 1813.
(8) Connell, J. G.; Richards, R. W.; Rennie, A. R. *Polymer* **1991**, *32*, 2033.
(9) Cahn, J. W.; Hilliard, J. E. *J. Chem. Phys.* **1958**, *28*, 258; **1959**, *31*, 688. Cahn, J. W. *J. Chem. Phys.* **1965**, *42*, 93.
(10) Snyder, H. L.; Meakin, P. *J. Polym. Sci., Polym. Symp.* **1985**, *73*, 217.
(11) Cook, H. E. *Acta Metall.* **1970**, *18*, 297.
(12) Kwak, K. D.; Okada, M.; Nose, T. *Polymer* **1991**, *32*, 864.
(13) Chu, B.; Ying, Q.-C.; Linliu, K.; Xie, P.; Gao, T.; Li, Y.; Nose, T.; Okada, M. *Macromolecules* **1992**, *25*, 7382.
(14) Chu, B.; Wu, D.; Wu, C. *Rev. Sci. Instrum.* **1987**, *58*, 1158.
(15) de Gennes, P.-G. *Scaling Concepts in Polymer Physics*; Cornell University Press: Ithaca, NY, 1979; Chapter IV.
(16) Okada, M.; Han, C. C. *J. Chem. Phys.* **1986**, *85*, 5317.
(17) Meier, H.; Strobl, G. R. *Macromolecules* **1987**, *20*, 649.
(18) Han, C. C.; Bauer, B. J.; Clark, J. C.; Muroga, Y.; Matsushita, Y.; Okada, M.; Tran-cong, Q.; Sanchez, I. C. *Polymer* **1988**, *29*, 2002.
(19) Binder, K. *Phys. Rev. A* **1984**, *29*, 341; *Colloid Polym. Sci.* **1987**, *265*, 273.
(20) Strobl, G. R. *Macromolecules* **1985**, *18*, 558.
(21) Urban, G.; Strobl, G. R. *Colloid Polym. Sci.* **1988**, *266*, 398.
(22) Benmouna, M.; Fischer, E. W., submitted for publications.
(23) Eu, M.-D.; Ullman, R., unpublished work.
(24) Eu, M.-D.; Ullman, R.; Summerfield, G. C. *Polym. Prep. (Am. Chem. Soc., Div. Polym. Chem.)* **1991**, *32*, 402.
(25) Ferry, J. D. *Viscoelastic Properties of Polymers*, 2nd ed.; John Wiley: New York, 1970; p 318.
(26) Plazek, D. J. *J. Phys. Chem.* **1965**, *69*, 3480.
(27) Russell, T. P.; Hadziioannou, G.; Warburton, W. K. *Macromolecules* **1985**, *18*, 78.